Journal of Data Acquisition and Processing
ISSN: 1004-9037
https://sjcjycl.cn/
DOI: 10.5281/zenodo.776598

OBJECT IDENTIFICATION IN SENSOR DATA USING QUANTUM TECHNIQUES

[1]Sandip Vaijanath Kendre, [2]Anand Singh Rajawat, [3]Amol Potgantwar
[1]Ph.D Research scholar , School of Computer Science & Engineering & Technology, Sandip University, Nashik, Maharashtra , India
[2,3]Professor , School of Computer Science & Engineering & Technology, Sandip University, Nashik, Maharashtra , India
[1] sandipkendre@gmail.com, [2]anandsingh.rajawat@sandipuniversity.edu.in
[3] amol.potgantwar@sitrc.org.

ABSTRACT: The negative effect of geometric distortion can be largely eliminated with the correct geometric transformation, so that we can focus on the image content itself in the next study and recognition. For this reason, geometric transformations are often used as a preprocessing step in other image processing applications. In this paper, quantum algorithms are developed using the geometric transformation of the quantum image representation QIRHSI (HSI Color Space Based Quantum Image Representation), including two-point exchange, circular translation, flip transform, and orthogonal rotation. HSI (Hue-Saturation-Intensity) color space. The above geometric transformation is performed by a quantum circuit with simple quantum gates. Analyzing the complexity of the fundamental quantum gate required for the above geometric transformations, it can be seen that the general transformations (circle translation, inverse transformation, and right-angle rotation) are lower than local transformations (two-point shifts). The geometric transformation concept is used to facilitate the low complexity and high performance of quantum images.
Keywords: Quantum computation, quantum image sensor data, quantum geometric transformation, quantum circuit, quantum discrete transform, object identification.

I. INTRODUCTION

The combination of quantum mechanics and computer science gave birth to the new discipline of quantum computing [1]. According to the new calculation it is possible to solve the failure of Moore's Law [1]. Quantum computing is very useful [2], it mainly occurs in quantum coherence, entanglement and overlapping of quantum states, which makes quantum computing more efficient than computation compared to data storage and computation. Thus, quantum computing can solve the inefficiencies of traditional solutions. Shor's polynomial-time algorithm [3] for solving differential equations and Grover's quadratic accelerated database search algorithm [4] in 1994 are the most famous examples.

These examples provide strong evidence for the superiority of quantum computers over classical computers. The fundamental problem of quantum imaging research is quantum imaging representation [5], [6], [7], [8], [9], [10], [11], [12], [13], [14 , [15], [16], [17], [18], [19], [20], [21], [22], [23]. Includes standard quantum image representation (see Table 1), Qubit Lattice [5], Real Ket [6], Mixed Image [7], Representation of Simple Quantum Images (FRQI) [8], Multi-Channel Representation for Quantum Image (MCRQI)) [9], New Enhanced

Quantum Representation (NEQR)[10], Normal Arbitrary Quantum Superposition State (NAQSS)[11], Color Quantum Display

TABLE 1. The different quantum image representation models.

QIR	Year	Inventor(s)	Required qubits	Color encoding	Complexity	Retrieval
QLM [5]	2003	Venegas-Andraca	2^{2n}	1 angle vectors (grayscale/RGB)		
RKM [6]	2005	Latorre	–	quantum superposition		
Entangled Image [7]	2010	Venegas-Andraca	–	binary geometrical shapes		
FRQI [8]	2011	Le	$2n+1$	1 angle vectors (grayscale)	$O(2^{4n})$	Probabilistic
MCRQI [9]	2011	Sun	$2n+3$	4 angle vectors (RGB)	$O(2^{4n+6})$	Probabilistic
NEQR [10]	2013	Zhang	$2n+q$	q qubits sequence (grayscale)		Deterministic
NAQSS [11]	2014	Li	$2n+1$	1 angle vectors (grayscale/RGB)		Probabilistic
CQIPT [12]	2014	Song	$2n+3$	4 angle vectors (RGB)		Probabilistic
FQRCI [13]	2014	Yang	$2n+3$	3 angle vectors(RGB)	$O(3\cdot 2^{4n})$	Probabilistic
SQR [14]	2014	Yuan	$2n+q+2$	1 angle vectors(infrared)	$O(2^{2n})$	Probabilistic
GQIR [15]	2015	Jiang	$h+w+q$	q qubits sequence (grayscale)	$O(2^{4n+2}+qn2^{2n})$	Deterministic
NCQI [16]	2016	Sang	$2n+3q$	$3q$ qubits sequence (RGB)		Deterministic
BRQI [17]	2018	Li	$2n+4$ / $2n+6$	q / $3q$ qubits sequence (grayscale/RGB)		Deterministic
OQIM [18]	2019	Xu		1 angle vectors (grayscale)		Probabilistic
QRCI [19]	2019	Wang	$2n+2$			Deterministic
	2020	Grigoryan	$2n+6$	q qubits sequence (RGB)		Probabilistic
FTQR [20]	2021	Yan	$r+s$	Fourier transform representation (grayscale/ RGB)		Probabilistic/ Deterministic
QHSL [21]	2022	Chen	$2n+q+1$	1 angle vectors and q qubits sequence (HSL)	$O(2^{4n+2}+qn2^{2n})$	Probabilistic/ Deterministic
QIRHSI [22]			$2n+q+2$	2 angle vectors and q qubits sequence (HSI)		

Phase shift (CQIPT) [12], modified color quantum representation (FQRCI) [13], simple quantum representation (SQR) [14], generalized quantum representation (GQIR) [15], new quantum representation Quantum representation of color digital images (NCQI)) [16], bit-plane representation of quantum images (BRQI) [17], sequentially encoded quantum image model (OQIM) [18], quantum representation model of color digital images (QRCI) [19], Fourier transform qubit representation (FTQR) [20], quantum hue, saturation and lightness (QHSL) [21], HSI color space based quantum image representation (QIRHSI) [22], etc. [15] tells us that there are currently two main research methods in quantum image processing: one is making representations of quantum images as shown in the previous paragraph, and the other is making algorithms based on quantum images. and list eight image processing algorithms: Simple Geometric Transformation [24], [25], [26], [27], image translation [28], [29], image scaling [15], [30], [31], [32], [33], color transformation [9], [10], [12], [16], [34], image scrambling [35], [36], [37], [38], image segmentation [7], [39], [40], [41], feature extraction [42], [43], quantum image watermarking [44], [45], [46], [47], [48], [49], [50], [51], [52], [53], image encryption [54], [55] , [56], [57] and quantum image encryption [58], [59], [60], [61], [62], [63], [64], [65], [66], [67], [68], [69], [70].

Coordinate transformations and geometric image modifications such as local translation, inversion, reflection, stretching and rotation require highly spatially varying systems [71]. Polynomial interpolator formulas can be used for efficient geometric transformation of 2D and 3D images in conventional computer systems [72]. Many applications such as medical analysis, biomedical systems and image guidance require the use of geometric image transformation techniques [73].

Geometric transformation [24], [25], [26], [27], [28], [29] is an important part of image processing and image analysis, but is still in its infancy for quantum images. Lee et al.

Fast geometric transformations based on FRQI notations [24] have been proposed, for example, two-point variation, rotation, joint exchange, orthogonal rotation, and their quantum variants using quantum gates, NOT, CNOT, and Toffoli Gate. The following year, Le et al. Three ideas have been proposed, including transforming subblocks in quantum images, extending the separation of classical operations to quantum transformations, and focusing on the smoothness of transformations that may not exist [25].

achieved using any of the earlier mentioned strategies. It is then used to construct new geometric transformations on FRQI quantum images form other transformations. In 2015, Wang, Jiang and Wang studied quantum image translations for the first time [28]. The entire and cyclic translation operations were proposed and quantum circuits for each of the two types of translation were given. In 2016, Fan et al. designed a new quantum algorithm to implement geometric transformations [26] based on Normal Arbitrary Superposi- tion State (NASS) of n qubits, including two-point swapping, symmetric flip, local flip, orthogonal rotations and transla- tions. In 2017, Zhou, Tan and Ian designed global translation and local translation based on quantum image FRQI [29]. The global translation is implemented using adder modulo N , and the local translation is implemented using Gray code, including single column translation, multi-column transla- tion and translation of restricted areas. In the same year, Yan et al. proposed a new method for quantum image rotation based on the NEQR quantum image shear trans- formation [27]. The horizontal and vertical shear mapping required to compute the rotation was accomplished by design- ing three basic computational units, namely quantum self- adder, quantum control multiplier and quantum interpolation circuit.

Nowadays, there are two research directions based on geometric transformations of quantum image representations. One direction is to study more general geometric transforma- tions based on quantum image representations, Zhang et al. proposed the affine transformation and the rotation trans- formation of arbitrary angle under the QUAntum Log-Polar Image (QUALPI) [74]. Based on the Flexible Log-Polar Image (FLPI) [75], an arbitrary rotational transformation was designed by Wang et al. The other direction is to study other operations on existing geometric transformations of quantum image representations, such as encryption, watermarking, etc. Zhou et al. in 2012 combined a variety of geometric transformations of quantum images to achieve encryption of quantum images, and also proposed two basic important contents: quantum grayscale image representation and quan- tum grayscale geometric transformation [76]. In 2014, Song et al. proposed a quantum image encryption scheme based on constrained geometric and color transformations [77]. In addition to this, Iliyasu et al. proposed a quantum computer image security based on restricted geometric

transform with no key, blind watermarking and authentication strategy [45]. The above results show that there is a great need to explore the research in this direction.

Inspired by the quantum geometric transformation algo- rithms based on quantum image representations FRQI and NASS, we designed the geometric transformation algo- rithm for quantum image representation QIRHSI. Firstly, the quantum geometric transformation algorithm of FRQI is for grayscale images, the geometric transformation algo- rithm of NASS is for multi-dimensional images, and our designed quantum geometric transformation algorithm based on QIRHSI is constructed for color images. Sec- ondly, it can better blend the quantum image representa- tion QIRHSI-based geometric transformation algorithm into other quantum image algorithms, such as image encryp- tion and image watermarking. Finally, the HSI model divides the image into color and grayscale information, making it more suitable for many grayscale processing techniques.

We use identify gates, NOT gates and multi-controlled not- gates as basic tools and aim to extend the use of quantum image representation models for different quantum image processing operations. The primary contribution of this paper is to give quantum geometric transformations based on the quantum image representation QIRHSI. In this paper, we analyze the complexity of quantum circuits using NOT gates and CNOT gates as the basic units.

(1) Based on the QIRHSI model, definition of the two- point swapping, circular translation, flipping transformation and right-angle rotation of the unitary operator are given, and the corresponding quantum circuits are given to analyze the complexity of different quantum geometric transformation operations in the form of theorems.

(2) The complexity of the quantum gates needed for differ- ent quantum geometry algorithms based on QIRHSI, FRQI and NAQSS models are compared, which corroborates from the side that the complexity of quantum geometry algorithms are closely related to the image size, but independent of the image color information.

The remainder of this paper is organized as follows. Section II introduces prior knowledge, with the basic quan- tum gates, the quantum color image representation QIRHSI, the plain adder and adder modulo N . Section III discusses in detail the geometric transformations based on QIRHSI images, including two-point swapping, circular translation, flipping transformations and right-angle rotation. The com- plexity comparison of the geometric transformations under different quantum image representation models are presented in Section IV. Experimental examples of the QIRHSI geo- metric transformation are given in Section V. The limi- tations of the geometric transformation algorithm are dis- cussed in Section VI. Conclusions and future outlook are in Section VII.

II. PRIOR KNOWLEDGE

A. BASIC QUANTUM GATES

First, we give some basic quantum gates to describe the geometric transformation of the quantum image, as depicted in Figure 1. These circuits are executed from left to right, and each line in the circuit represents a wire. A quantum circuit is equivalent to the operation of a unitary matrix.

B. QIRHSI REPRESENTATION

We review how QIRHSI [22] represents a color image based on HSI color space. QIRHSI is an outstanding representation of quantum color images, which is derived from FRQI [8]

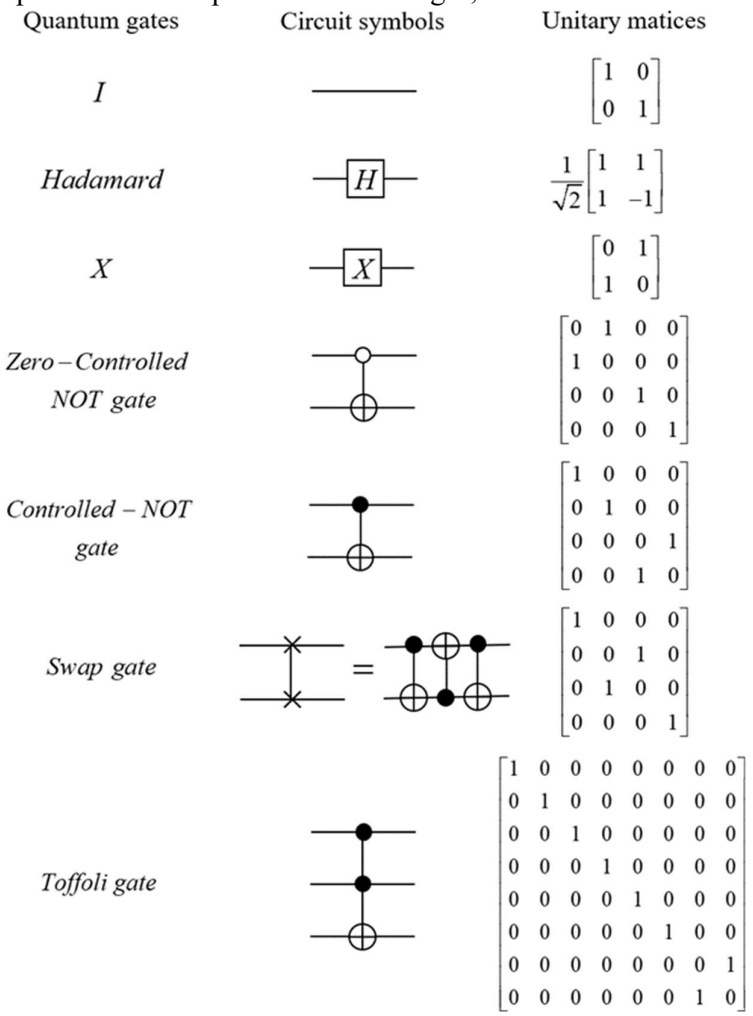

FIGURE 1. Some quantum basic gates, circuit symbols and corresponding unitary matrices.

and NEQR [10] model. According to the QIRHSI model, the quantum color image can be described as shown in Eq. (1).

$$
\begin{aligned}
|I(\vartheta)\rangle &= \frac{1}{2^n}\sum_{k=0}^{2^{2n}-1} |c_k\rangle \otimes |k\rangle \\
&= \frac{1}{2^n}\sum_{k=0}^{2^{2n}-1} |H_k\rangle\,|S_k\rangle\,|I_k\rangle \otimes |k\rangle \\
&= \frac{1}{2^n}\sum_{y=0}^{2^n-1}\sum_{x=0}^{2^n-1} \cdot H_{yx}\ \cdot S_{yx}\ \cdot I_{yx} \otimes |yx\rangle \qquad (1)
\end{aligned}
$$

wherein,

$$|H_k\rangle = \cos \vartheta_{hk} |0\rangle + \sin \vartheta_{hk} |1\rangle$$
$$|S_k\rangle = \cos \vartheta_{sk} |0\rangle + \sin \vartheta_{sk} |1\rangle$$
$$|I_k\rangle = .C_k^0 C_k^1 \ldots C_k^{q-2} C_k^{q-1}$$

$$\vartheta_{hk}, \vartheta_{sk} \in \left[0, 2^{-1}\pi\right], \quad C_k^m \in \{0, 1\}$$
$$m = 0, 1, \ldots, q-1$$
$$k = yx = 0, 1, \ldots, 2^{2n} - 1$$

i.e. |Ck ⟩ and |yx⟩ encode the color information and location
information of the quantum color image, respectively. |y⟩ = yn−1 . . . y1y0 signifies the first n-qubits along the vertical axis and x xn 1 . . . x1x0 signifies the last n-qubits along the horizontal axis. A 4 4 color image and QIRHSI quantum state representation is provided in Figure 2.

C. PLAIN ADDER

To calculate the sum of the two numbers stored in the two

|Hk ⟩ = cos θhk |0⟩ + sin θhk |1⟩
|Sk ⟩ = cos θsk |0⟩ + sin θsk |1⟩
|Ik ⟩ = .C C . . . C C

quantum registers a and b , it is necessary to rely on plain adder [78], [79].
Addition can be written in the following form.
|a, b, 0⟩ → |a, b, a + b⟩

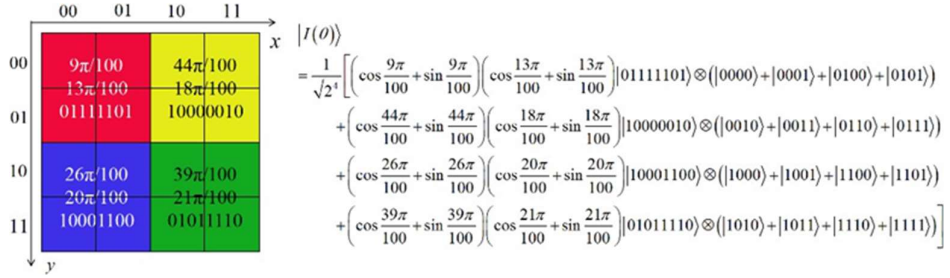

FIGURE 2. A 4 × 4 color image and QIRHSI quantum state representation.

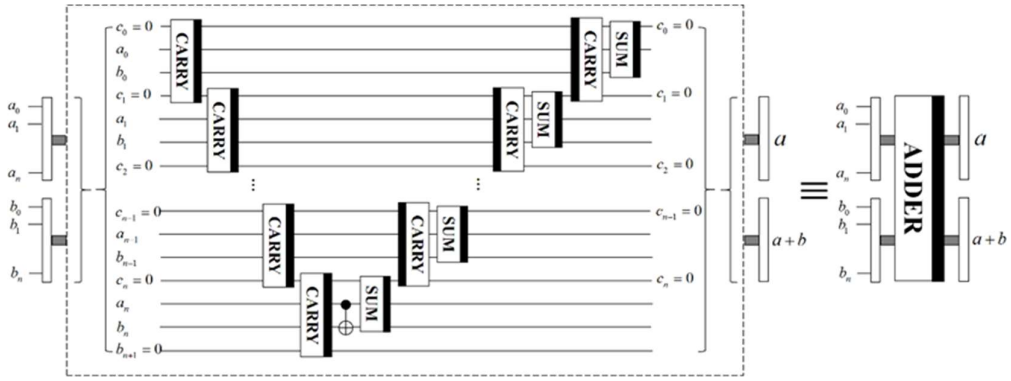

FIGURE 3. Plain adder network.

Rewrites the result of the calculation to one of the input registers, i.e.

$|a, b\rangle \rightarrow |a, a + b\rangle$ (2)

Figure 3 presents the network structure of the plain adder, where the sub-networks for the basic carry and sum opera- tions are shown in Figure 4.

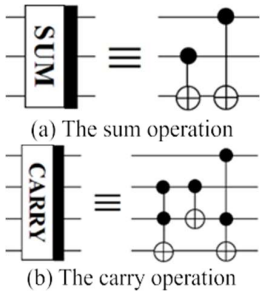

(a) The sum operation

(b) The carry operation

where a, b [0, N). The quantum network structure of the adder modulo N is provided in Figure 5.

III. GEOMETRIC TRANSFORMATION OF QIRHSI IMAGE Geometric transformations of the quantum grayscale image FRQI (two-point swapping, flipping, coordinate swapping and orthogonal rotation) [24] and the quantum color image NASS (two-point swapping, symmetric flip, local flip, orthogonal rotation and translation) [26] have been inves- tigated so far. Based on these results, we have researched the geometric transformations of the quantum color image of QIRHSI [22], including two-point swapping, circular translation, flip transformation and right-angle rotation. Therefore, the general geometric transformation based on the quantum color image QIRHSI is defined as

$$G_T\left(|I(\vartheta)\rangle\right) = \frac{1}{2^n} \sum_{k=0}^{2^{2n}-1} |H_k\rangle|S_k\rangle|I_k\rangle \otimes G\left(|k\rangle\right) \qquad (4)$$

FIGURE 4. Basic sum and carry operation.

D. ADDER MODULO N

The adder modulo N is a quantum network that is commonly used to calculate the modulo sum of two numbers [78], [79]. Its explicit form is illustrated in Eq. (3).

$|a, b\rangle \rightarrow |a, (a + b) \mod N\rangle$ (3)

where I (θ) represents a QIRHSI quantum color image as shown in Eq. (1). The operator GT for general geometric transformations can also be written as

$GT = I \otimes 2 \otimes I \otimes q \otimes G$ (5)

The quantum circuits of the general geometric transforma- tion operator GT based on the quantum color image QIRHSI are given in Figure 6.

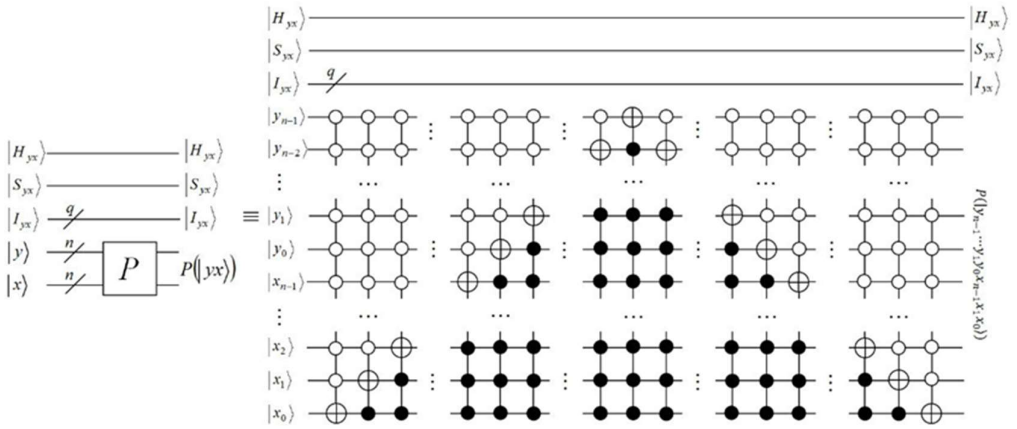

FIGURE 7. The quantum circuit of QIRHSI color images implementing the two-point swap of pixels i 0 and .j = .22n − 1E.

Because more than one Gray code connecting i and j always exists, there is no unique that implements the swap between the two pixels of i and j [1]. For example, for i 0010 and j 1111, two Gray codes are shown in Eqs. (12) and (13).

0 0 1 0
0 0 1 1
0 1 1 1
1 1 1 1

and

0 0 1 0
1 0 1 0
1 1 1 0
1 1 1 1

Theorem 1: The complexity of the quantum gate required to implement the two-point swap operator GP on the quantum image QIRHSI using Gray codes is O n2 .

Proof of Theorem 1: Let the pixel positions to be swapped in the quantum image QIRHSI by the two-point swapping operator GP are i and j , and the elements of a set of Gray codes connecting 2n bits of binary numbers i and j to g1, g2, . . . , gm 1, gm, where g1 0, gm 22n 1. The state transformations are implemented step by step using simply a series of quantum gates

$|g1\rangle \rightarrow |g2\rangle \rightarrow \ldots \rightarrow |gm-1\rangle$

then multi-controlled NOT gate operations are conducted, followed by transformations

$|g1\rangle \rightarrow |g2\rangle \rightarrow \ldots \rightarrow |gm-1\rangle$

the final result is the two-point swap operator GP imple- mented in quantum circuits, with the required quantum gate complexity of O n2 [1], [80]. In the following we will start

The first step is to swap the states of g1 and g2 . Let g1 and g2 have different values for the lth bit, then we can complete the swap by flipping one of the controlled bits of the lth qubit, the condition to be satisfied is that the both
|g1⟩ and |g2⟩ have the same qubit for the rest of the bits. Next, use a controlled operation to swap |g2⟩ and |g3⟩, and so on, until |gm−2⟩ and |gm−1⟩ have been swapped. The above m − 2 operations complete the operations in Eq. (14)

$$|g1\rangle \rightarrow |gm-1\rangle$$
$$|g2\rangle \rightarrow |g1\rangle$$
$$|g3\rangle \rightarrow |g2\rangle$$
$$\ldots$$
$$|gm-1\rangle \rightarrow |gm-2\rangle \qquad (14)$$

It should be noted that all other states of the computational basis remain unchanged during the sequence of operations. In the second step, let the w th bits of gm 1 and gm are different, and under the condition that the other bits of gm 1 and gm are the same, conduct a multi-control NOT gate operation targeting the wth qubit. Finally, the reductive swap operation is used to complete the multi-control NOT gate operation: gm−1 and gm−2 are swapped, followed by gm 2 and gm 3 , and so on, until g2 and g1 are swapped.

Since i and j differ in at most 2n positions, it can always find a Gray code that satisfies m 2n 1 [1]. To imple- ment the two-stage unitary operation up to 2 (2n 1) con- trolled not-gate operations are required to swap g1 to gm 1 and back again. And each such controlled operation can be implemented using O (n) NOT gates and multi control oper- ation NOT gates. The achievement of a multi-control NOT gate operation with the wth qubit as the target also requires O (n) elementary quantum gates. Thus, the implementation of |g1 ⟩ to |gm−1⟩ requires the quantum elementary gate of gate required for the quantum circuit implementation of the two-point swap operator GP on QIRHSI is O n2 .

A. CIRCULAR TRANSLATIONS

The circular translation of the QIRHSI image along the coordinate axis is described in Definition 2. Figure 8 gives an example of a circular translation of the image along the coordinate axis.

(a) Original Tree image (b) Circular translation along the y-axis (c) Circular translation along the x-axis

FIGURE 8. The image Tree was cyclically translated along the coordinate axis.

Definition 2: The operators Ty l and Tx l based on QIRHSI color image translated by l pixels along the y and x axis respectively are defined as
Ty+l (|I (θ)⟩)
2n−1 2n−1

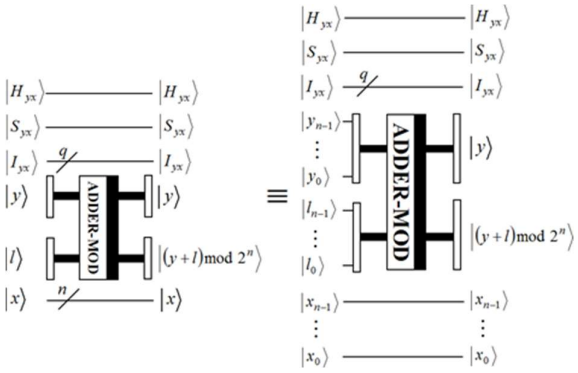

FIGURE 9. Quantum circuit of the QIRHSI image translated by l pixels along the y axis.

= 1 X X .Hyx .Syx .Iyx ⊗ .(y + l) mod 2n, x (15)

Tx+l (|I (θ)⟩)
1 2n−1 2n−1
= .Hyx .Syx .Iyx ⊗ .y, (x + l) mod 2 (16)

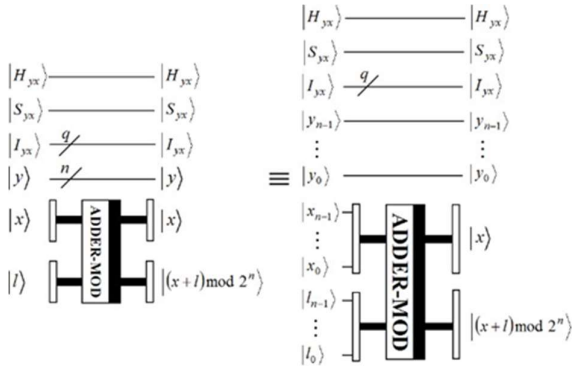

FIGURE 10. Quantum circuit of the QIRHSI image translated by *l* pixelsalong the *x* axis.

Theorem 2: The complexity of the quantum gates needed for the circular translation operators T and T on the

whereby |I (θ)⟩ represents a QIRHSI color image, see Eq. (1). l = ln−1 . . . l1l0 and l ∈ (0, 2n − 1],
so li (i = 0, 1, . . . , n − 1) is not all zero. The translation oper-

Proof of Theorem 2: In ordered to calculate the number
of quantum gates required for the circular translation opera- tors Ty+l and Tx+l, it is only needed to calculate the number of

ators Ty+l and Tx+l can be expressed respectively as

$$T_{y+l} = I^{\otimes 2} \otimes I^{\otimes q} \otimes \sum_{j=0}^{2n-1} |(j+l) \bmod 2n\rangle\langle j| \otimes I^{\otimes n} = I^{\otimes 2} \otimes I^{\otimes q}$$

quantum elementary gates required for the module 2n adder. As one Toffoli gate is equivalent to six CNOT gates [78]. In the basic carry and sum operation (see Figure 4), the number of CNOT gates taken is 13 and 2 respectively. And the plain adder (see Figure 3) contains 2n 1 carries, n sums and 1 CNOT gate, so the number of CNOT gates required for

$$\otimes \left(|0\rangle\langle 0| + \sum_{l=1}^{2n-1} |(2n-1+l) \bmod 2n\rangle\langle 2n-1| \right) \otimes I^{\otimes n} \quad (17)$$

the plain adder is 28n 12. The linear relationship with the input n of the quantum circuit.
The module 2n adder (see Figure 5) contains 5 plain adders, 2 NOT gates and up to 2n + 4 CNOT gates. Thus, the module 2n adder needs 2 NOT gates and up to 142n − 56 CNOT

$$T_{x+l} = I^{\otimes 2} \otimes I^{\otimes q} \otimes I^{\otimes n} \otimes \sum_{j=0}^{} (j+l) \bmod 2n\langle j| = I^{\otimes 2} \otimes I^{\otimes q} \otimes I^{\otimes n}$$

gates, i.e. the complexity of the quantum gates required for the module 2n adder is O (n). That is, the complexity of the quantum gates required for the circular translation operators

$$|(0+l) \bmod 2n\rangle\langle 0| + \ldots + |(2n-1+l) \bmod 2n\rangle\langle 2n-1| \quad (18)$$

T_{y+l} and T_{x+l} is O (n).

B. FLIP TRANSFORMATIONS

The quantum circuits of the circular translation operators
T_{y+l} and T_{x+l} are given in Figures 9 and 10.

The flip transformation of the QIRHSI image along the coordinate axis is shown in Definition 3. Figure 11 gives

an example of the image flipping transformation along the coordinate axis.

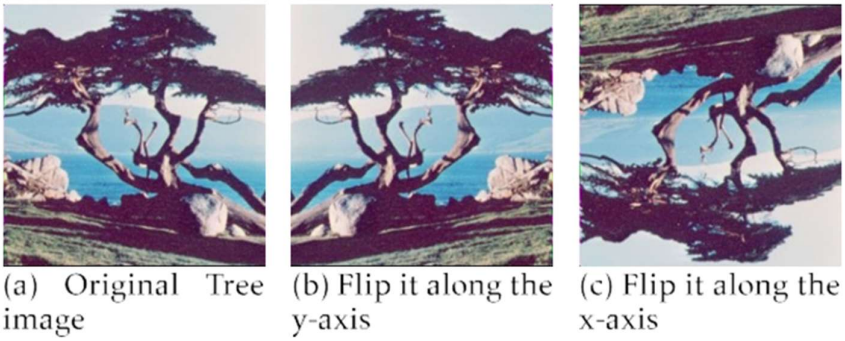

(a) Original Tree image (b) Flip it along the y-axis (c) Flip it along the x-axis

FIGURE 11. The image Tree was flipped along the coordinate axis.

Definition 3: The QIRHSI color image based flip transfor- mation operators Fy and Fx along the y and x axis respec- tively are defined as

Fy (|I (θ)⟩)

2n−1 2n−1

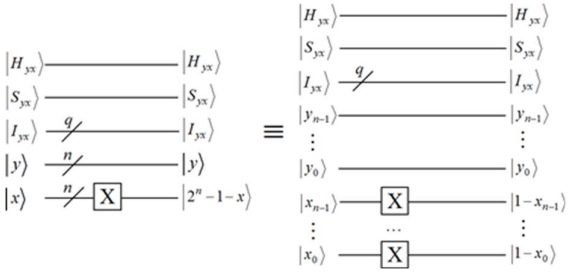

FIGURE 12. QIRHSI color image of the quantum circuit flipped along the y -axis.

1

= 2n

X X .Hyx .Syx .Iyx ⊗ |yx¯⟩

y=0 x=0

1

= 2n

2n−1 2n−1

.Hyx

.Syx

.Iyx

⊗ .y, 2n − 1 − x (19)

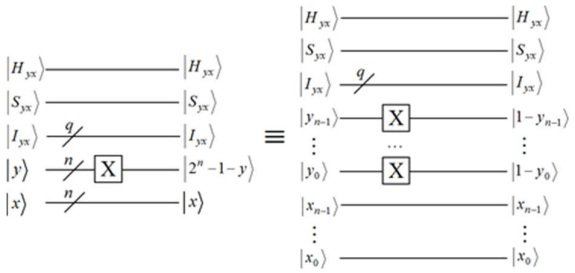

FIGURE 13. QIRHSI color image of the quantum circuit flipped along the x -axis.

y=0
Fx (|I (θ)⟩)

x=0

the quantum gates required to implement the flip operators Fy

1 2n−1 2n−1
= .Hyx .Syx .Iyx ⊗ |y¯x⟩

and Fx on the QIRHSI image is O (n).

n n
= 1 X X .Hyx .Syx .Iyx ⊗ .2n − 1 − y, x (20)

y = −x axis as shown in Definition 4. Figure 14 shown an example of the image flipping transformation along the y = x

where I (θ) represents a QIRHSI color image, see Eq. (1). And

|y⟩ = |yn−1 . . . y1y0⟩
|x⟩ = |xn−1 . . . x1x0⟩
y yn 1 . . . y1y0 2 1 y
|x¯⟩ = |x¯n−1 . . . x¯1x¯0⟩ = 2n − 1 − x y¯i = 1 − yi, x¯i = 1 − xi
i = 0, 1, . . . , n − 1
The flip transformation operators Fy and Fx are denoted as
Fy = I ⊗2 ⊗ I ⊗q ⊗ I ⊗n ⊗ X ⊗n (21)
Fx = I ⊗2 ⊗ I ⊗q ⊗ X ⊗n ⊗ I ⊗n (22)
The quantum circuits of the flipping transform operators

FIGURE 14. The image Tree is transformed by flipping along the y = x and y = −x axis.

Definition 4: The QIRHSI color image based flipping operators Fy x and Fy x along the y x and y x axis respectively are defined as
Fy=x (|I (θ)⟩)

Fy and Fx are shown in Figures 12 and 13.

1 2n−1 2n−1
= .Hyx .Syx .Iyx ⊗ V (|yx⟩)

tum image QIRHSI is O (n).
Proof of Theorem 3: The flip operators Fy and Fx are

1
= 2n

2n−1 2n−1
.Hyx .Syx .Iyx ⊗ |xy⟩(23)

shown in Eqs. (21) and (22), and it can be seen that both operators Fy and Fx use n NOT gates, so the complexity of

y=0 x=0
Fy=−x (|I (θ)⟩)

1 2n−1 2n−1
= .Hyx .Syx .Iyx ⊗ |x¯y¯⟩

Theorem 4: The complexity of the quantum gates needed

n n
= 1 X X .Hyx .Syx .Iyx ⊗ .2n − 1 − x, 2n − 1 − y

Proof of Theorem 4: The flipping operators Fy x and
F

2n
y=0

x=0

(24)

y=−x are shown in Eqs. (25) and (26), which show that the operator Fy x uses n swap gates, and the operator Fy x uses 2n NOT gates and n swap gates. Because one swap gate is equivalent to three CNOT gates [1], the complexity of the

whereby I (θ) represents a QIRHSI color image, see Eq. (1). The flip transformation operators Fy x and Fy x can be expressed respectively as

Fy=x = I ⊗2 ⊗ I ⊗q ⊗ V (25)

Fy=−x = Fy=x FyFx (26)

The quantum circuits of the flip transformation operators Fy x and Fy x are shown in Figures 15 and 16, and the quantum circuit of the operator V is given in Figure 17.

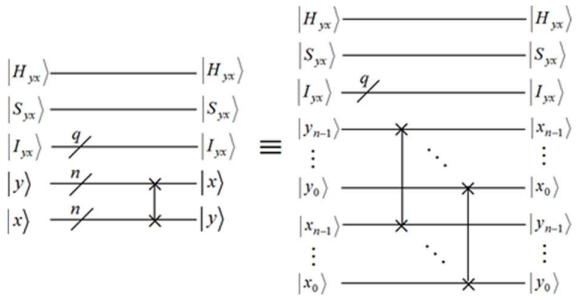

FIGURE 15. QIRHSI image of a flipped quantum circuit along the y x axis.

quantum gates needed to implement the flipping operators Fy=x and Fy=−x on the QIRHSI is O (n).

C. RIGHT-ANGLE ROTATIONS

The transformation of the QIRHSI image rotation angle to π/2, π and 3π/2 are shown in Definition 5. Figure 18 shows an example of the transformation with image rotation angles π/2, π and 3π/2.

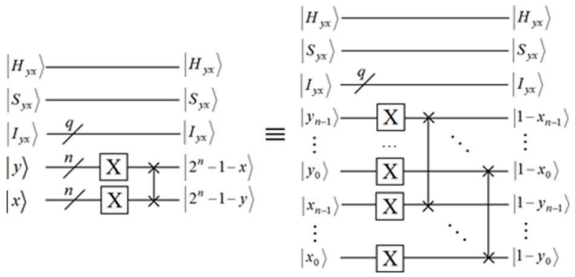

FIGURE 16. QIRHSI image of a flipped quantum circuit along the y x axis.

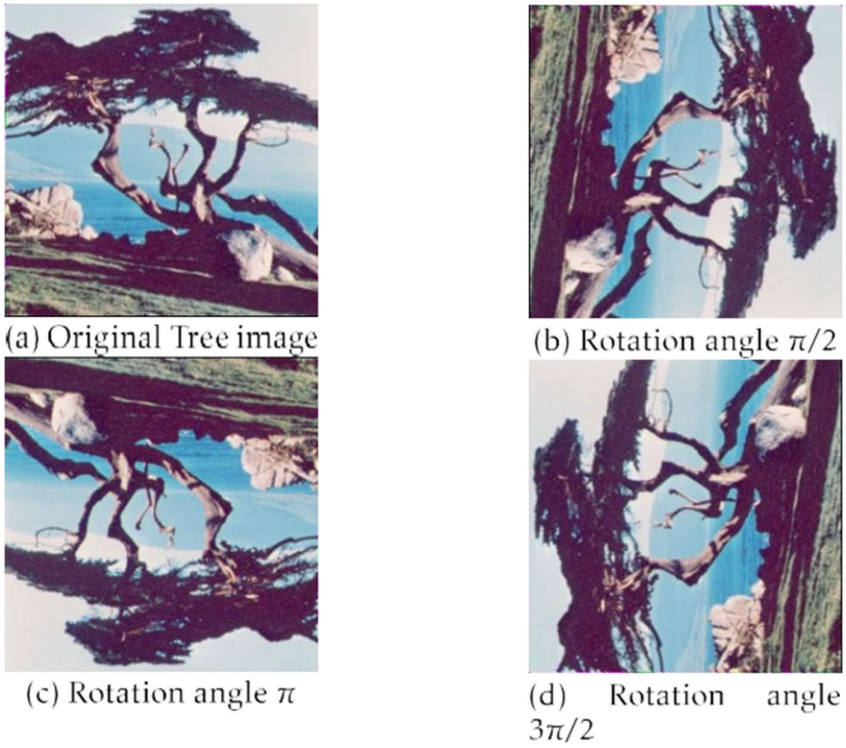

FIGURE 18. Image Tree and right angle after rotation.

Definition 5: The right angle rotation operators Rπ/2, Rπ and R3π/2 based on QIRHSI color image rotation angles of π/2, π and 3π/2 transformations are defined as

Rπ/2 (|I (θ)⟩)
2n−1 2n−1

1
= 2n

X X .Hyx .Syx .Iyx ⊗ |xy¯⟩

y=0 x=0

$$= \frac{1}{2^n}$$

$$\sum_{x=0}^{n}\sum_{y=0}^{n} .H_{yx} .S_{yx} .I_{yx} \otimes .x, 2n-1-y \quad (27)$$

$$R_\pi (|I(\theta)\rangle)$$

$$= \frac{1}{2^n} \sum_{x=0}^{2n-1}\sum_{y=0}^{2n-1} .H_{yx} .S_{yx} .I_{yx} \otimes |\bar{y}\bar{x}\rangle$$

$$= \frac{1}{2^n}$$

$$\sum_{x=0}^{n}\sum_{y=0}^{n} .H_{yx} .S_{yx} .I_{yx} \otimes .2n-1-y, 2n-1-x$$

(28)

$$R_{3\pi/2} (|I(\theta)\rangle)$$

$$= \frac{1}{2^n} \sum_{x=0}^{2n-1}\sum_{y=0}^{2n-1} .H_{yx} .S_{yx} .I_{yx} \otimes |\bar{x}\bar{y}\rangle$$

$$= \frac{1}{2^n}$$

$$\sum_{x=0}^{n}\sum_{y=0}^{n} .H_{yx} .S_{yx} .I_{yx} \otimes .2n-1-x, y \quad (29)$$

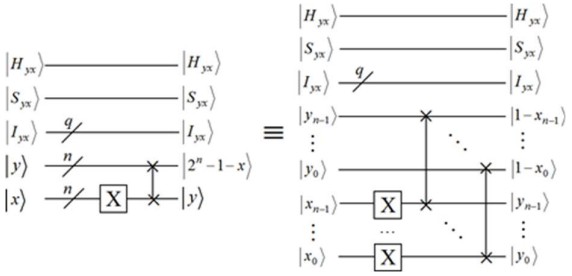

FIGURE 21. QIRHSI image of the quantum circuit with a rotation angle of 3π/2.

where I (θ) represents a QIRHSI color image, see Eq. (1). The right-angle rotation operators Rπ/2, Rπ and R3π/2 can be expressed respectively as

Rπ/2 = Fy=xFx (30)

Rπ = FyFx (31)

R3π/2 = Fy=x Fy (32)

The quantum circuits of the operators Rπ/2, Rπ and R3π/2 are shown in Figures 19, 20 and 21.

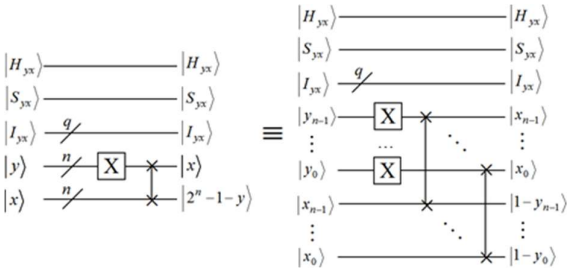

FIGURE 19. QIRHSI image of the quantum circuit with a rotation angle of π/2.

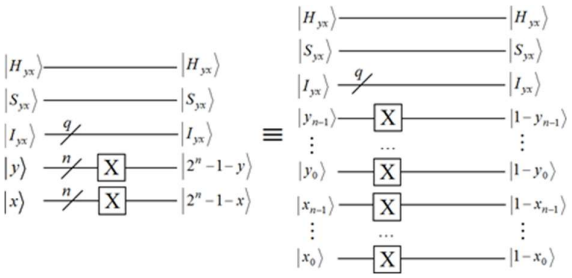

FIGURE 20. QIRHSI image of the quantum circuit with a rotation angle of π .

Theorem 5: The complexity of the quantum gates required for the right-angle rotation operators Rπ/2, Rπ and R3π/2 on the quantum image QIRHSI is O (n).

Proof of Theorem 5: The right-angle rotation operators Rπ/2, Rπ and R3π/2 are shown in Eqs. (30), (31) and (32), and it can be known that the operator Rπ/2 uses n NOT gates and n swap gates, the operator Rπ uses n NOT gates, and the operator R3π/2 uses n NOT gates and n swap gates. Thus, the complexity of the quantum gates needed to implement the right-angle rotation operators Rπ/2, Rπ and R3π/2 on the QIRHSI is O (n).

IV. COMPARISON OF THE COMPLEXITY OF QUANTUM GEOMETRIC TRANSFORMATIONS

The geometric transformation of quantum images has been
a highly interesting research topic for scholars. As yet, geometric transformations based on the two-dimensional quantum gray-scale image FRQI [24] and geometric transfor- mations based on the multidimensional quantum color image NASS [26] are the two ways that can be used. Table 2 gives the complexity of the quantum gates needed for the geometric transformation operations based on the quantum image repre- sentation models FRQI, NASS and QIRHSI. It was indicated that this table compares images of size 2n × 2n.

TABLE 2. The complexity of the quantum gates required for geometric transformations based on different quantum image models is compared.

Geometric transfor- mations	Based on QIRHSI rep- resentation	Based on NASS repre- sentation	Based on FRQI repre- sentation
Two-point swap	$O(n^2)$	$O(n^2)$	$O(n^2)$
Circular translations	$O(n)$	$O(2^n n^2)$	–
Flip transforma- tions	$O(n)$	$O(n)$	$O(n)$
Right-angle rotations	$O(n)$	$O(n)$	$O(n)$

As can be seen from Table 2, the quantum gray-scale image FRQI involved no circular translation, while the complexity O (n) of quantum gates required for the quantum circular translation operation designed in this paper based on the quantum 2D color image QIRHSI is much lower than the complexity O 2nn2 of the quantum circular translation oper- ation designed based on the quantum multi-dimensional color image NASS.

In classical computers, the global operators of geomet- ric transformations require 22n matrices to be implemented, therefore the complexity of the implemented operations are at least O 22n . However, in quantum systems, no matter for quantum image representation FRQI, NASS and QIRHSI, quantum global transform operations (circular translation, flipping transform and right-angle rotation) require less com- plexity of quantum gates than local transform operations are swapped. The corresponding quantum circuits are given in Figure 24. The two-point swap operator GP is defined as

G I ⊗2 I ⊗8 P

□□ |1⟩ ⟨11| + |11⟩ ⟨1| + □□

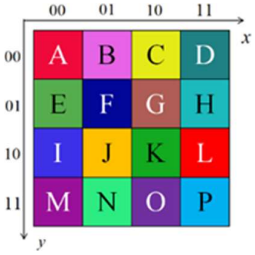

(two-point swapping), which are required to be implemented by O (n) quantum gates, and the reason for this result is due to the parallelism of quantum computing. Therefore, quan- tum geometric transformation techniques based on quantum image representation FRQI, NASS and QIRHSI are applied to image encryption [70], [81], watermarking [47] and so on.

= I ⊗2 ⊗ I ⊗8 ⊗

15
 k=0,k≠1,11

|k⟩ ⟨k|

(34)

V. EXPERIMENTAL EXAMPLE OF THE QIRHSI GEOMETRIC TRANSFORMATIONS

In order to make the geometric transformation based on the
QIRHSI image more visual, a quantum color image QIRHSI of size 4 4, where n 2 and q 8, is shown in Figure 22 as an example. A 4 4 color image of QIRHSI is given in Figure 22 and is represented in Eq. (33).
24−1

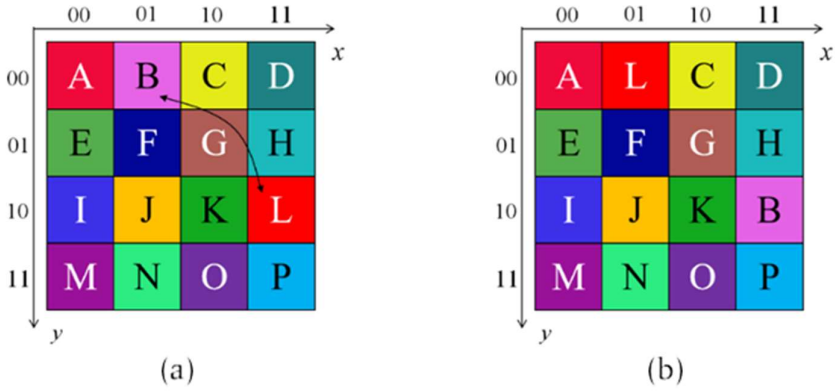

FIGURE 23. (a) Original image; (b) After the two-point swap.

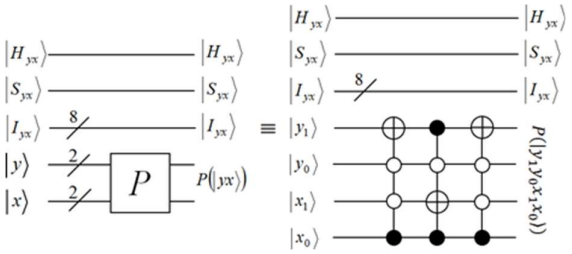

FIGURE 24. The quantum circuit for two-point swapping.

1
|I (θ)⟩ = 22

|Hk ⟩ |Sk ⟩ |Ik ⟩ ⊗ |k⟩
k=0

Applying Eq. (34) to image |I (θ)⟩ gives
G (|I (θ)⟩)

2 2 P
= 1 X X .Hyx .Syx .Iyx ⊗ |yx⟩ (33) 1 X
|H11⟩ |S11⟩ |I11⟩ ⊗ |1⟩ + |H1⟩ |S1⟩ |I1⟩ ⊗ |11⟩ □□□

= 4 □□ +

k=0X,k≠1,11

|Hk ⟩ |Sk ⟩ |Ik ⟩ ⊗ |k⟩ □□

FIGURE 22. A 4 × 4 color image of QIRHSI.

A. TWO-POINT SWAP

Figure 23 gives an example of a QIRHSI color image where two pixels |i⟩=|1⟩ = |00⟩|01⟩ and |j⟩ = |11⟩ = |10⟩|11⟩

where P (|k⟩) = |k⟩, k ≠ 1, 11, and P (|1⟩) = |11⟩,

Observing Figure 23, it can be seen that we swapped the two pixels labeled with the alphabets B and L, corresponding to the pixel positions 1 and 11, respectively. From the quan- tum circuit shown in Figure 24, it can be seen that swapping pixel positions 1 and 11 requires six NOT gates and three controlled not-gates. Since one three-controlled not-gate is equivalent to four Toffoli gates, one Toffoli gate is equiv- alent to six controlled not-gates. Therefore, swapping pixel locations 1 and 11 needs six NOT gates and 72 controlled not-gates.

B. CIRCULAR TRANSLATION

An example of circular translation of a QIRHSI color image along the x-axis is given in Figure 25, where l 3. The corresponding quantum circuit are given in Figure 26. The circular translation operator Tx+3 is defined as

3
Tx+3 = I ⊗2 ⊗ I ⊗8 ⊗ I ⊗2 ⊗ |(j + 3) mod 4⟩ ⟨j|
j=0

FIGURE 23. (a) Original image; (b) After the two-point swap.

= I ⊗2 ⊗ I ⊗8 ⊗ I ⊗2
⊗ (|3⟩ ⟨0| + |0⟩ ⟨1| + |1⟩ ⟨2| + |2⟩ ⟨3|)

Applying the circular translation operator Tx+3 to the image |I (θ)⟩ to obtain
3 3

T (I (θ)) 1 H S I y, (x 3) mod 4 4 y=0 x=0
Obviously, it is a circular translation of Figure 22 by 3 pixels along the positive direction of the x-axis to obtain Figure 25(b). Analysis of the quantum circuit shown in Figure 26 shows that the use of a module 4 adder is equiv- alent to the use of 5 plain, 2 NOT gates and no more than 8 controlled not-gates (See Theorem 2). In other words, the circular translation of 3 pixels along the positive direction of the x-axis uses 5 NOT gates and 228 controlled not-gates.

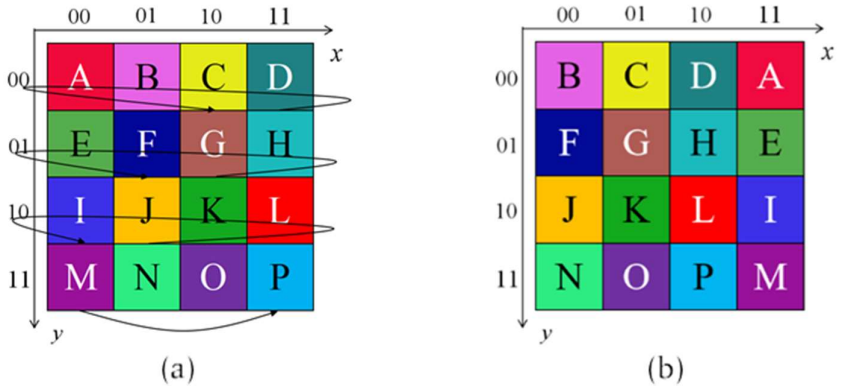

FIGURE 25. (a) Original image; (b) After circular translation.

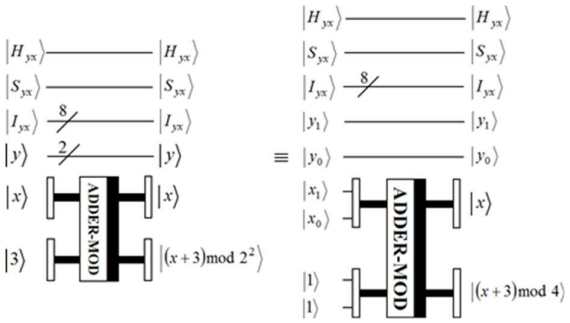

FIGURE 26. Quantum circuits of circular translations.

C. FLIP TRANSFORMATION

Figure 27 gives an example of a QIRHSI color image flipped along the x axis. The corresponding quantum circuits are shown in Figure 28.
The flip transformation operator Fx is described by the definition of
Fx = I ⊗2 ⊗ I ⊗8 ⊗ X ⊗2 ⊗ I ⊗2
Applying the flip transformation operator Fx to the image
|I (θ)⟩ gives

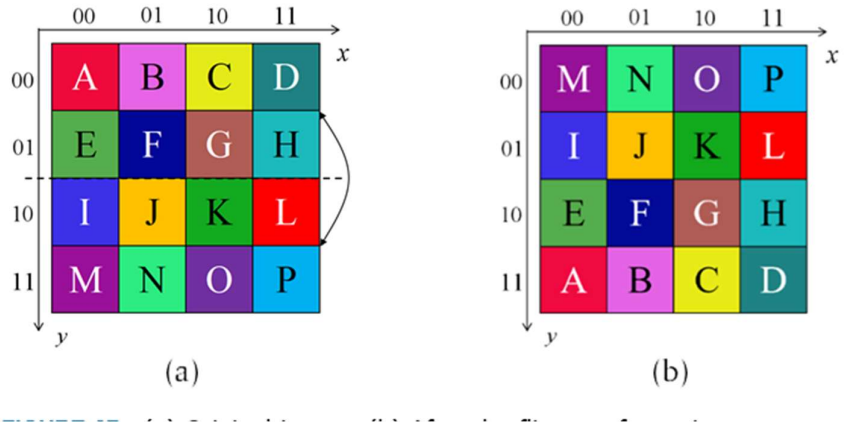

FIGURE 27. (a) Original image; (b) After the flip transformation.

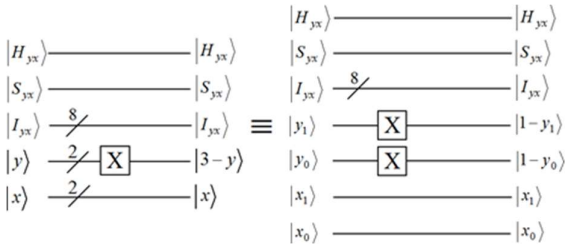

FIGURE 28. The quantum circuit of the flip transformation along the x axis.

Obviously, a flipping transformation of Figure 22 along the x-axis to obtain Figure 27(b) requires only 2 NOT gates (see Figure 28).

D. FLIP TRANSFORMATION

An example of a QIRHSI color image flipped transformation along the y x axis is given in Figure 29. Figure 30 gives the corresponding quantum circuits.

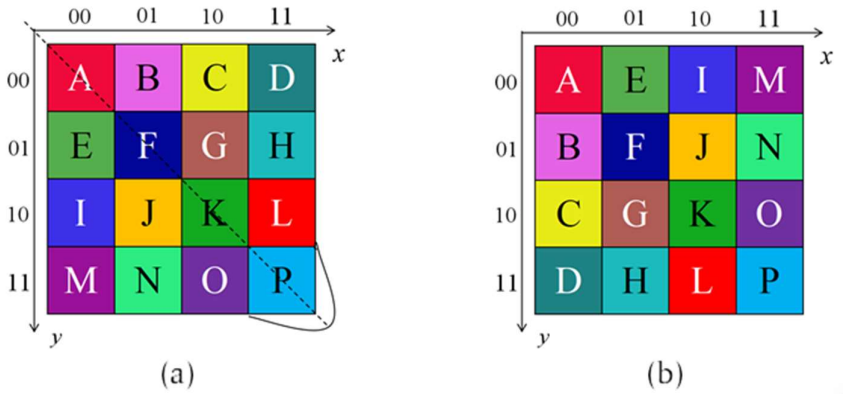

FIGURE 29. (a) Original image; (b) After flipping along the y = x axis.

The flip transformation operator Fy=x defined as
Fy=x = I ⊗2 ⊗ I ⊗8 ⊗ V
where the operator V is shown in Figure 31.
The flip transformation operator Fy=x is applied to the image |I (θ)⟩ to obtain

3 3 3 3
Fx (|I (θ)⟩) = 1 X X .Hyx .Syx .Iyx ⊗ |3 − y, x⟩ Fy=x (|I (θ)⟩) = 1 X X .Hyx .Syx .Iyx ⊗ |xy⟩

operator Rπ/2 is
Rπ/2 = Fy=x Fx
Applying the right-angle rotation operator Rπ/2 to the image |I (θ)⟩ gives
3 3

R (|I (θ)⟩) = 1 X X .H

.S

.I

⊗ |x, 3 − y⟩

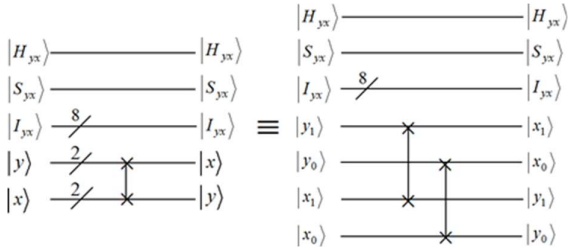

FIGURE 30. The quantum circuit flipped along the y = x axis.

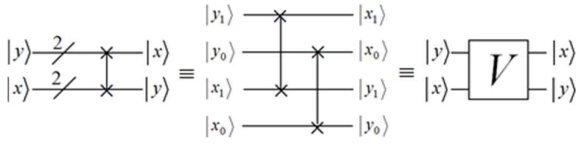

FIGURE 31. Quantum circuit of the operator V .

The flipping transformation of Figure 22 along the y x axis results in Figure 29(b), which requires only two swap gates to complete the operation (see Figure 30). One swap gate is equivalent to three controlled not-gates. Therefore, six controlled not-gates are needed for the flipping transforma- tion operation along the y = x axis.

E. RIGHT-ANGLE ROTATION

An example of a QIRHSI color image rotated an angle of π/2 is given in Figure 32. The corresponding quantum circuits are provided in Figure 33. The right-angle rotation

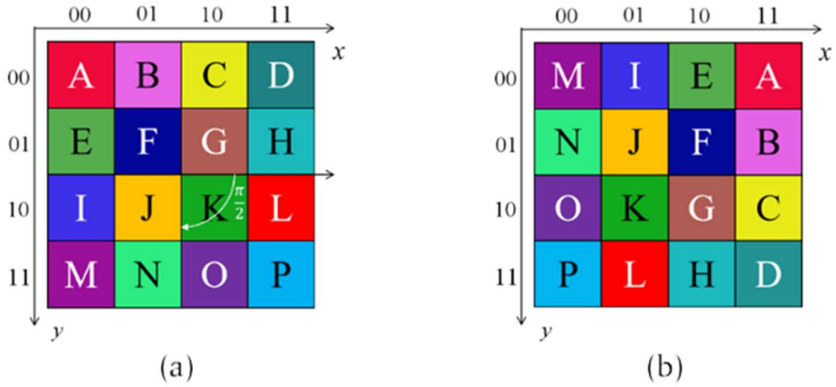

FIGURE 32. (a) Original image; (b) After rotation π/2.

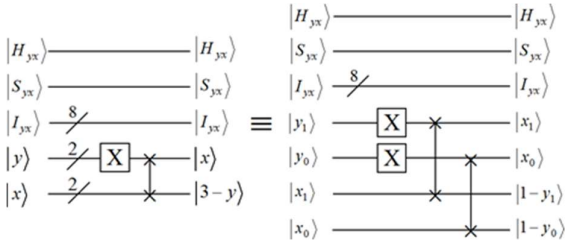

FIGURE 33. The quantum circuit of rotated π/2.

Rotating Figure 22 by π/2 to obtain Figure 32(b), only two
NOT gates and two swap gates are needed (see Figure 33), i.e., only two NOT gates and six controlled not-gates are needed to complete this operation.

VI. CONCLUSION AND FUTURE OUTLOOK

In this paper, quantum geometric transformations based on the quantum color image QIRHSI are proposed, covering two-point swapping, circular translation, flipping transforma- tions and right-angle rotation. The quantum circuits for the four types of geometric transformation operations mentioned above are designed immediately afterwards, and the com- plexity analysis of the quantum gates needed for the differ- ent types of geometric transformation unitary operators are given. The complexity of the global transformation (circular translation, flipping transformation and right-angle rotation) operator of the quantum color image QIRHSI is lower than with the local transformation (two-point swapping) operator. Finally, the quantum geometric transformation operation of QIRHSI color image is illustrated by a simple 4 4 example.

The future research work covers

1) The circular transformations, flipping transformations and right-angle rotations covered in this paper are whole geometric transformations, and it is essential to implement local circular translations, local flipping transformations and local right-angle rotations.

2) Flipping transformations (along the y axis, x axis, y x axis and y x axis) and right-angle rotations (π/2, π and 3π/2) are both special quantum geometric trans- formations and how to design flipping transformations along the arbitrary axis and rotating transformations at arbitrary angles.

3) How to design general translation operations in the field of quantum image processing after designing cir- cular translation operations with modulo N adder.
4) How to construct arbitrary geometric transformations using the two-point swapping operator, while making the designed quantum circuits for arbitrary geometric transformations with lower complexity is still a prob- lem to be further considered.
5) Additional applications in quantum image process- ing combined with quantum geometric transformations are of higher value, for example, in quantum image encryption, where pixel position scrambling in quan- tum image encryption can be accomplished by combining sequences generated by chaotic mapping with quantum circuits.
6) In practical applications, how to better use quan- tum geometric transformations to correction of images taken by artificial satellites and how to use quantum geometric transformations to processing satellite cloud images commonly used in weather forecast, etc.

REFERENCES

[1] M. A. Nielsen and I. L. Chuang, Quantum Computation and Quantum Information. Cambridge, U.K.: Cambridge Univ. Press, 2010.
[2] R. P. Feynman, ‘‘Simulating physics with computers,’’ Int. J. Theor. Phys., vol. 21, nos. 6–7, pp. 467–488, 1982.
[3] P. W. Shor, ‘‘Algorithms for quantum computation: Discrete logarithms and factoring,’’ in Proc. 35th Annu. Symp. Found. Comput. Sci., 1994, pp. 124–134.
[4] L. K. Grover, ‘‘A fast quantum mechanical algorithm for database search,’’ in Proc. 28th Annu. ACM Symp. Theory Comput., 1996, pp. 212–219.
[5] S. E. Venegas-Andraca and S. Bose, ‘‘Storing, processing, and retrieving an image using quantum mechanics,’’ Proc. SPIE, vol. 5105, pp. 137–147, Aug. 2003.
[6] J. I. Latorre, ‘‘Image compression and entanglement,’’ Quantum Phys., pp. 1–4, Oct. 2005. [Online]. Available: https://arxiv.53yu.com/abs/quant- ph/0510031
[7] S. E. Venegas-Andraca and J. L. Ball, ‘‘Processing images in entan- gled quantum systems,’’ Quantum Inf. Process., vol. 9, no. 1, pp. 1–11, Feb. 2010.
[8] P. Q. Le, F. Dong, and K. Hirota, ‘‘A flexible representation of quantum images for polynomial preparation, image compression, and processing operations,’’ Quantum Inf. Process., vol. 10, no. 1, pp. 63–84, 2012.
[9] B. Sun, P. Q. Le, A. M. Iliyasu, F. Yan, J. A. Garcia, F. Dong, and K. Hirota, ‘‘A multi-channel representation for images on quantum computers using the RGBα color space,’’ in Proc. IEEE 7th Int. Symp. Intell. Signal Pro- cess., Sep. 2011, pp. 19–21.
[10] Y. Zhang, K. Lu, Y. Gao, and M. Wang, ‘‘NEQR: A novel enhanced quantum representation of digital images,’’ Quantum Inf. Process., vol. 12, no. 8, pp. 2833–2860, 2013.
[11] H.-S. Li, Q. Zhu, R.-G. Zhou, L. Song, and X.-J. Yang, ‘‘Multi-dimensional color image storage and retrieval for a normal arbitrary quantum superpo- sition state,’’ Quantum Inf. Process., vol. 13, no. 4, pp. 991–1011, 2014.
[12] X. Song, S. Wang, and X. Niu, ‘‘Multi-channel quantum image represen- tation based on phase transform and elementary transformations,’’ J. Inf. Hiding Multimedia Signal Process., vol. 5, no. 4, pp. 574–585, 2014.

[13] Y.-G. Yang, X. Jia, S.-J. Sun, and Q.-X. Pan, ‘‘Quantum cryptographic algorithm for color images using quantum Fourier transform and double random-phase encoding,’’ Inf. Sci., vol. 277, pp. 445–457, Sep. 2014.
[14] S. Yuan, X. Mao, Y. Xue, L. Chen, Q. Xiong, and A. Compare, ‘‘SQR: A simple quantum representation of infrared images,’’ Quantum Inf. Pro- cess., vol. 13, no. 6, pp. 1353–1379, 2014.
[15] N. Jiang, J. Wang, and Y. Mu, ‘‘Quantum image scaling up based on nearest-neighbor interpolation with integer scaling ratio,’’ Quantum Inf. Process., vol. 14, no. 11, pp. 4001–4026, Nov. 2015.
[16] J. Sang, S. Wang, and Q. Li, ‘‘A novel quantum representation of color digital images,’’ Quantum Inf. Process., vol. 16, no. 2, pp. 1–14, Feb. 2017.
[17] H.-S. Li, X. Chen, H. Xia, Y. Liang, and Z. Zhou, ‘‘A quantum image representation based on bitplanes,’’ IEEE Access, vol. 6, pp. 62396–62404, 2018.
[18] G. Xu, X. Xu, X. Wang, and X. Wang, ‘‘Order-encoded quantum image model and parallel histogram specification,’’ Quantum Inf. Process., vol. 18, no. 11, pp. 1–26, Nov. 2019.
[19] L. Wang, Q. Ran, J. Ma, S. Yu, and L. Tan, ‘‘QRCI: A new quantum representation model of color digital images,’’ Opt. Commun., vol. 438, pp. 147–158, May 2019.
[20] A. M. Grigoryan and S. S. Agaian, ‘‘New look on quantum representa- tion of images: Fourier transform representation,’’ Quantum Inf. Process., vol. 19, no. 5, pp. 1–26, May 2020.
[21] F. Yan, N. Li, and K. Hirota, ‘‘QHSL: A quantum hue, saturation, and lightness color model,’’ Inf. Sci., vol. 577, pp. 196–213, Oct. 2021.
[22] G.-L. Chen, X.-H. Song, S. E. Venegas-Andraca, and A. A. A. El-Latif, ‘‘QIRHSI: Novel quantum image representation based on HSI color space model,’’ Quantum Inf. Process., vol. 21, no. 1, pp. 1–31, Jan. 2022.
[23] M. Lisnichenko and S. Protasov, ‘‘Quantum image representation: A review,’’ Quantum Mach. Intell., vol. 5, no. 1, pp. 1–2, Jun. 2023.
[24] P. Q. Le, A. M. Iliyasu, F. Dong, and K. Hirota, ‘‘Fast geometric transfor- mations on quantum images,’’ IAENG Int. J. Appl. Math., vol. 40, no. 3, pp. 1–2, 2010.
[25] P. Q. Le, A. M. Iliyasu, F. Dong, and K. Hirota, ‘‘Strategies for designing geometric transformations on quantum images,’’ Theor. Comput. Sci., vol. 412, pp. 1406–1418, Mar. 2011.
[26] P. Fan, R.-G. Zhou, N. Jing, and H.-S. Li, ‘‘Geometric transformations of multidimensional color images based on NASS,’’ Inf. Sci., vols. 340–341, pp. 191–208, May 2016.
[27] F. Yan, K. Chen, S. E. Venegas-Andraca, and J. Zhao, ‘‘Quantum image rotation by an arbitrary angle,’’ Quantum Inf. Process., vol. 16, no. 11, p. 282, Nov. 2017.
[28] J. Wang, N. Jiang, and L. Wang, ‘‘Quantum image translation,’’ Quantum Inf. Process., vol. 14, no. 5, pp. 1589–1604, May 2015.
[29] R.-G. Zhou, C. Tan, and H. Ian, ‘‘Global and local translation designs of quantum image based on FRQI,’’ Int. J. Theor. Phys., vol. 56, no. 4, pp. 1382–1398, Apr. 2017.
[30] N. Jiang and L. Wang, ‘‘Quantum image scaling using nearest neighbor interpolation,’’ Quantum Inf. Process., vol. 14, no. 5, pp. 1559–1571, 2015.

[31] J. Sang, S. Wang, and X. Niu, ‘‘Quantum realization of the nearest- neighbor interpolation method for FRQI and NEQR,’’ Quantum Inf. Pro- cess., vol. 15, no. 1, pp. 37–64, Jan. 2016.
[32] P. Li and X. Liu, ‘‘Bilinear interpolation method for quantum images based on quantum Fourier transform,’’ Int. J. Quantum Inf., vol. 16, no. 4, Jun. 2018, Art. no. 1850031.
[33] R.-G. Zhou, Y. Cheng, X. Qi, H. Yu, and N. Jiang, ‘‘Asymmetric scaling scheme over the two dimensions of a quantum image,’’ Quantum Inf. Process., vol. 19, no. 9, p. 343, Sep. 2020.
[34] P. Q. Le, A. M. Iliyasu, F. Dong, and K. Hirota, ‘‘Efficient color transforma- tions on quantum images,’’ J. Adv. Comput. Intell. Intell. Inform., vol. 15, no. 6, pp. 698–706, 2011.
[35] N. Jiang, W.-Y. Wu, and L. Wang, ‘‘The quantum realization of Arnold and Fibonacci image scrambling,’’ Quantum Inf. Process., vol. 13, no. 5, pp. 1223–1236, May 2014.
[36] N. Jiang and L. Wang, ‘‘Analysis and improvement of the quantum Arnold image scrambling,’’ Quantum Inf. Process., vol. 13, no. 7, pp. 1545–1551, Jul. 2014.
[37] N. Jiang, L. Wang, and W.-Y. Wu, ‘‘Quantum Hilbert image scrambling,’’
Int. J. Theor. Phys., vol. 53, no. 7, pp. 2463–2484, 2014.
[38] R.-G. Zhou, Y.-J. Sun, and P. Fan, ‘‘Quantum image gray-code and bit- plane scrambling,’’ Quantum Inf. Process., vol. 14, no. 5, pp. 1717–1734, 2015.
[39] S. Caraiman and V. I. Manta, ‘‘Image segmentation on a quantum com- puter,’’ Quantum Inf. Process., vol. 14, no. 5, pp. 1693–1715, May 2015.
[40] P. Li, T. Shi, Y. Zhao, and A. Lu, ‘‘Design of threshold segmenta- tion method for quantum image,’’ Int. J. Theor. Phys., vol. 59, no. 2, pp. 514–538, Feb. 2020.
[41] S. Yuan, C. Wen, B. Hang, and Y. Gong, ‘‘The dual-threshold quantum image segmentation algorithm and its simulation,’’ Quantum Inf. Process., vol. 19, no. 12, p. 425, Dec. 2020.
[42] Y. Zhang, K. Lu, K. Xu, Y. Gao, and R. Wilson, ‘‘Local feature point extraction for quantum images,’’ Quantum Inf. Process., vol. 14, no. 5, pp. 1573–1588, May 2015.
[43] N. Jiang, Z. Ji, H. Li, and J. Wang, ‘‘Quantum image interest point extraction,’’ Mod. Phys. Lett. A, vol. 36, no. 9, Mar. 2021, Art. no. 2150063.
[44] W.-W. Zhang, F. Gao, B. Liu, H.-Y. Jia, Q.-Y. Wen, and H. Chen, ‘‘A quan- tum watermark protocol,’’ Int. J. Theor. Phys., vol. 52, no. 2, pp. 504–513, Feb. 2013.
[45] A. M. Iliyasu, P. Q. Le, F. Dong, and K. Hirota, ‘‘Watermarking and authentication of quantum images based on restricted geometric transfor- mations,’’ Inf. Sci., vol. 186, no. 1, pp. 126–149, 2012.
[46] Y.-G. Yang, X. Jia, P. Xu, and J. Tian, ‘‘Analysis and improvement of the watermark strategy for quantum images based on quantum Fourier trans- form,’’ Quantum Inf. Process., vol. 12, no. 8, pp. 2765–2769, Aug. 2013.
[47] X.-H. Song, S. Wang, S. Liu, A. A. A. El-Latif, and X.-M. Niu, ‘‘A dynamic watermarking scheme for quantum images using quantum wavelet trans- form,’’ Quantum Inf. Process., vol. 12, no. 12, pp. 3689–3706, 2013.
[48] F. Yan, A. M. Iliyasu, B. Sun, S. E. Venegas-Andraca, F. Dong, and
K. Hirota, ‘‘A duple watermarking strategy for multi-channel quantum images,’’ Quantum Inf. Process., vol. 14, no. 5, pp. 1675–1692, 2015.
[49] S. Heidari and M. Naseri, ‘‘A novel LSB based quantum watermarking,’’

Int. J. Theor. Phys., vol. 55, no. 10, pp. 4205–4218, 2016.
[50] P. Li, Y. Zhao, H. Xiao, and M. Cao, ‘‘An improved quantum watermarking scheme using small-scale quantum circuits and color scrambling,’’ Quan- tum Inf. Process., vol. 16, no. 5, p. 127, 2017.
[51] Y.-G. Yang, J. Xia, X. Jia, and H. Zhang, ‘‘Novel image encryp- tion/decryption based on quantum Fourier transform and double phase encoding,’’ Quantum Inf. Process., vol. 12, no. 11, pp. 3477–3493, 2013.
[52] D. Awasthi and V. K. Srivastava, ‘‘Robust, imperceptible and opti- mized watermarking of DICOM image using Schur decomposition, LWT-DCT-SVD and its authentication using SURF,’’ Multimedia Tools Appl., vol. 2022, pp. 1–35, Sep. 2022.
[53] S. Iranmanesh, R. Atta, and M. Ghanbari, ‘‘Implementation of a quantum image watermarking scheme using NEQR on IBM quantum experience,’’ Quantum Inf. Process., vol. 21, no. 6, p. 194, Jun. 2022.
[54] A. Ullah, A. A. Shah, J. S. Khan, M. Sajjad, W. Boulila, A. Akgul,
J. Masood, F. A. Ghaleb, S. A. Shah, and J. Ahmad, ‘‘An efficient lightweight image encryption scheme using multichaos,’’ Secur. Commun. Netw., vol. 2022, pp. 1–16, Oct. 2022.
[55] Y. Y. Ghadi, S. A. Alsuhibany, J. Ahmad, H. Kumar, W. Boulila,
M. Alsaedi, K. Khan, and S. A. Bhatti, ‘‘Multi-chaos-based lightweight image encryption-compression for secure occupancy monitoring,’’
J. Healthcare Eng., vol. 2022, pp. 1–14, Nov. 2022.
[56] F. Ahmed, M. U. Rehman, J. Ahmad, M. S. Khan, W. Boulila,
G. Srivastava, J. C.-W. Lin, and W. J. Buchanan, ‘‘A DNA based colour image encryption scheme using a convolutional autoencoder,’’ ACM Trans. Multimedia Comput., Commun., Appl., vol. 2022, pp. 1–22, Nov. 2022.
[57] F. Masood, J. Masood, L. Zhang, S. S. Jamal, W. Boulila, S. U. Rehman,
F. A. Khan, and J. Ahmad, ‘‘A new color image encryption technique using DNA computing and Chaos-based substitution box,’’ Soft Comput., vol. 26, pp. 1–17, Apr. 2021.
[58] T. Hua, J. Chen, D. Pei, W. Zhang, and N. Zhou, ‘‘Quantum image encryp- tion algorithm based on image correlation decomposition,’’ Int. J. Theor. Phys., vol. 54, pp. 526–537, Feb. 2015.
[59] N. R. Zhou, T. X. Hua, L. H. Gong, D. J. Pei, and Q. H. Liao, ‘‘Quan- tum image encryption based on generalized Arnold transform and dou- ble random-phase encoding,’’ Quantum Inf. Process., vol. 14, no. 4, pp. 1193–1213, 2015.
[60] L.-H. Gong, X.-T. He, S. Cheng, T.-X. Hua, and N.-R. Zhou, ‘‘Quantum image encryption algorithm based on quantum image XOR operations,’’ Int. J. Theor. Phys., vol. 55, no. 7, pp. 3234–3250, Jul. 2016.
[61] L. Li, B. Abd-El-Atty, A. A. El-Latif, and A. Ghoneim, ‘‘Quantum color image encryption based on multiple discrete chaotic systems,’’ in Proc. Federated Conf. Comput. Sci. Inf. Syst., Sep. 2017, pp. 3–6.
[62] L.-H. Gong, X.-T. He, R.-C. Tan, and Z.-H. Zhou, ‘‘Single channel quan- tum color image encryption algorithm based on HSI model and quan- tum Fourier transform,’’ Int. J. Theor. Phys., vol. 57, no. 1, pp. 59–73, Jan. 2018.

[63] Q. W. Ran, S. Yu, L. Wang, and J. Ma, ‘‘A quantum color image encryption scheme based on coupled hyper-chaotic Lorenz system with three impulse injections,’’ Quantum Inf. Process., vol. 17, no. 8, p. 188, 2018.
[64] A. A. A. El-Latif, B. Abd-El-Atty, S. E. Venegas-Andraca, and
W. Mazurczyk, ‘‘Efficient quantum-based security protocols for informa- tion sharing and data protection in 5G networks,’’ Future Gener. Comput. Syst., vol. 100, pp. 893–906, Nov. 2019.
[65] A. A. A. El-Latif, B. Abd-El-Atty, and S. E. Venegas-Andraca, ‘‘Controlled alternate quantum walk-based pseudo-random number generator and its application to quantum color image encryption,’’ Phys. A, Stat. Mech. Appl., vol. 547, Jun. 2020, Art. no. 123869.
[66] B. Abd-El-Atty, A. A. Abd El-Latif, and S. E. Venegas-Andraca, ‘‘An encryption protocol for NEQR images based on one-particle quantum walks on a circle,’’ Quantum Inf. Process., vol. 18, no. 9, p. 272, Sep. 2019.
[67] X. Liu, D. Xiao, and C. Liu, ‘‘Three-level quantum image encryption based on Arnold transform and logistic map,’’ Quantum Inf. Process., vol. 20, no. 1, p. 23, Jan. 2021.
[68] U. Erkan, A. Toktas, and Q. Lai, ‘‘2D hyperchaotic system based on Schaffer function for image encryption,’’ Expert Syst. Appl., vol. 213, Mar. 2023, Art. no. 119076.
[69] U. Erkan, A. Toktas, F. Toktas, and F. Alenezid, ‘‘2D eπ -map for image encryption,’’ Inf. Sci., vol. 589, pp. 770–789, Apr. 2022.
[70] X. Song, G. Chen, and A. A. A. El-Latif, ‘‘Quantum color image encryption scheme based on geometric transformation and intensity channel diffu- sion,’’ Mathematics, vol. 10, no. 17, p. 3038, Aug. 2022.